

Modelling ammonia emission from urine patches

A. Móríng et al.

[Title Page](#)

[Abstract](#)

[Introduction](#)

[Conclusions](#)

[References](#)

[Tables](#)

[Figures](#)



[Back](#)

[Close](#)

[Full Screen / Esc](#)

[Printer-friendly Version](#)

[Interactive Discussion](#)



A process-based model for ammonia emission from urine patches, GAG (Generation of Ammonia from Grazing): description, validation and sensitivity analysis

A. Móríng^{1,2,3}, M. Vieno^{1,2}, R. M. Doherty¹, J. Laubach⁴, A. Taghizadeh-Toosi⁵, and M. A. Sutton²

¹University of Edinburgh, Crew Building, Alexander Crum Brown Road, Edinburgh, EH9 3FF, UK

²NERC, Centre for Ecology & Hydrology, Edinburgh, Bush Estate, Midlothian, Penicuik, EH26 0QB, UK

³Hungarian Meteorological Service, Kitaibel P. u. 1, 1024 Budapest, Hungary

⁴Landcare Research, P.O. Box 69040, Lincoln 7640, New Zealand

⁵Department of Agroecology, Aarhus University, Blichers Allé 20, 8830 Tjele, Denmark

Received: 29 May 2015 – Accepted: 08 June 2015 – Published: 08 July 2015

Correspondence to: A. Móríng (a.moring@sms.ed.ac.uk)

Published by Copernicus Publications on behalf of the European Geosciences Union.

BGD

12, 10059–10113, 2015

Modelling ammonia emission from urine patches

A. Móríng et al.

Title Page

Abstract

Introduction

Conclusions

References

Tables

Figures



Back

Close

Full Screen / Esc

Printer-friendly Version

Interactive Discussion



Abstract

In this paper a new process-based, weather-driven model for ammonia (NH_3) emission from a urine patch has been developed and its sensitivity to various factors assessed. This model, the GAG model (Generation of Ammonia from Grazing) was developed as a part of a suite of weather-driven NH_3 exchange models, as a necessary basis for assessing the effects of climate change on NH_3 related atmospheric processes.

GAG is capable of simulating the TAN (Total Ammoniacal Nitrogen) content, pH and the water content of the soil under a urine patch. To calculate the TAN budget, GAG takes into account urea hydrolysis as a TAN input and NH_3 volatilization as a loss. In the water budget, in addition to the water content of urine, precipitation and evaporation are also considered. In the pH module we assumed that the main regulating processes are the dissociation and dissolution equilibria related to the two products of urea hydrolysis: ammonium and bicarbonate. Finally, in the NH_3 exchange flux calculation we adapted a canopy compensation point model that accounts for exchange with soil pores and stomata as well as deposition to the leaf surface.

We validated our model against measurements, and carried out a sensitivity analysis. The validation showed that the simulated parameters (NH_3 exchange flux, soil pH, TAN budget and water budget) are well captured by the model ($r > 0.5$ for every parameter at $p < 0.01$ significance level). We found that process-based modelling of pH is necessary to reproduce the temporal development of NH_3 emission. In addition, our results suggested that more sophisticated simulation of CO_2 emission in the model could potentially improve the modelling of pH.

The sensitivity analysis highlighted the vital role of temperature in NH_3 exchange; however, presumably due to the TAN limitation, the GAG model currently provides only a modest overall temperature dependence in total NH_3 emission compared with the values in the literature.

BGD

12, 10059–10113, 2015

Modelling ammonia emission from urine patches

A. M3ring et al.

Title Page

Abstract

Introduction

Conclusions

References

Tables

Figures



Back

Close

Full Screen / Esc

Printer-friendly Version

Interactive Discussion



Since all the input parameters can be obtained for study at larger scales, GAG is potentially suitable for larger scale application, such as in regional atmospheric and ecosystem models.

1 Introduction

The consequences of strong emission of reactive nitrogen compounds (N_r), dominated by the emission of ammonia (NH_3), are widely discussed: threatening air, water and soil quality, it endangers also ecosystems as well as human health in many ways (Sutton et al., 2011; Galloway et al., 2008; Fowler et al., 2013). Globally 70 % of NH_3 released to atmosphere originates from agricultural sources, such as livestock housing, manure management and fertilizer spreading on fields (EDGAR, 2011). According to the latest available report of the UK government agency DEFRA (Department for Environment Food and Rural Affairs), in the UK grazing accounts for ca. 11 % of the total NH_3 emission (Misselbrook et al., 2012). In spite of its small proportion of emission, since two thirds of the grasslands are estimated to be grazed (Hellsten et al., 2008), grazing affects a significant percentage of the country.

Ammonia exchange between atmosphere and surface, as it was confirmed by both laboratory and field experiments (Farquhar et al., 1980; Sutton et al., 1995), is a bidirectional process and dependent largely on meteorological factors, especially temperature. The direction of the net NH_3 exchange at any time depends on the relative magnitude of the ambient air concentration of NH_3 high above the surface and the concentration of NH_3 right above the surface (referred to as the “compensation point”). If the air concentration is the larger of the two, deposition occurs; whilst in the opposite case, emission takes place.

During grazing, the dominant NH_3 source is urine, rather than dung (Petersen et al., 1998; Laubach et al., 2013). In a urine patch ammonium (NH_4^+) is produced by urea hydrolysis. The process is catalysed by the enzyme urease, which is the product of several bacteria species, in the presence of water. To maintain the chemical equilibria

Modelling ammonia emission from urine patches

A. M3ring et al.

Title Page

Abstract

Introduction

Conclusions

References

Tables

Figures



Back

Close

Full Screen / Esc

Printer-friendly Version

Interactive Discussion



Modelling ammonia emission from urine patches

A. Móríng et al.

Title Page

Abstract

Introduction

Conclusions

References

Tables

Figures



Back

Close

Full Screen / Esc

Printer-friendly Version

Interactive Discussion



Several attempts have been made to simulate NH_3 emission from urine patches as well as grazed fields. Laubach et al. (2012) published an inverse NH_3 volatilization model from urine patches to calculate soil resistance, applying also a simple compensation point model. The equilibrium gaseous NH_3 concentration in the soil pores was considered as a compensation point, and three resistances (a soil, an aerodynamic, and a quasi-laminar resistance) were assumed between the soil and air concentration. Running the model in reverse mode, simulating NH_3 emission, requires soil sampling and measurement of pH and NH_4^+ concentration of soil water.

The approach for the process of urea hydrolysis in the above mentioned inverse model is based on the earlier model of Sherlock and Goh (1985), which accounts for the NH_3 volatilization from urine patches and aqueous urea. This model for describing the transfer of NH_3 between surface and atmosphere operates with a constant “volatilization exchange coefficient”, rather than a system of dynamically changing resistances. Rachhpal and Nye (1986) made an attempt to simulate NH_3 emission from applied urea. Although this model employed a constant “transfer coefficient” for NH_3 volatilization as well as a constant rate of urea hydrolysis were applied, the study gives an alternative for modelling the chemistry of a urine patch, as well as the vertical distribution of the different nitrogen compounds under the urine patch.

The present paper reports our work to construct and test a process-based, weather-driven model for NH_3 emission from a urine patch, which can be applied on both field and regional scales. As such, the development represents a contribution toward developing a comprehensive suite of weather-dependent ammonia exchange models, as a necessary basis for assessing the effects of climate change on ammonia emissions and deposition (Sutton et al., 2013). As soil measurements are not widely available, we had to account for the relevant processes in the soil, such as the change of concentration of the different reduced nitrogen compounds, pH and water content. On the other hand, bearing in mind our final goal – a detailed investigation of weather dependency of NH_3 emission from grazing – we focused predominantly on the parametrisation of

the effect of meteorological variables, keeping the simulation of physical and chemical soil processes as simple as possible.

In this paper we firstly provide the description of our model of Generation of Ammonia from Grazing (GAG). Then we present the results from the model validation based on the measurements by Laubach et al. (2012). Finally, we report the results of a sensitivity analysis in relation to the uncertain model parameters as well as several meteorological variables.

2 Description of the GAG model

To simulate NH_3 emission over a urine patch the GAG model calculates the TAN budget and the water budget, as well as the soil pH (hydrogen ion, H^+ , budget) under the patch. For this purpose, firstly, we assume that, during urination and rain events, the incoming liquid infiltrates the soil to fill soil pores until the wetted soil layer reaches its field capacity. After this point we neglect any further downward or upward motion (capillary rise) in the soil.

We also make the assumption that soil NH_3 emission occurs only from the “source layer”, the very top layer of the wetted soil column (similarly to Riedo et al., 2002), while reduced nitrogen (here the sum of NH_x and urea) that infiltrates beneath this layer is assumed to be nitrified. This assumption allows us to handle the numerous soil pores in the source layer as a single big pore – referred hereafter as “model soil pore” –, the liquid content of which represents the soil pores filled by liquid, while its gaseous section represents the air-filled soil pores in the source layer (Fig. 1). If more liquid (urine or rain water) gets into the soil than the model soil pore can hold (more than the water content of the source layer at field capacity), the excess infiltrates to the deeper soil layers.

The input to the TAN budget is generated by hydrolysis of the urea contained within incoming urine, while NH_3 emission acts as a loss from the TAN budget. Soil pH is also regulated by urea hydrolysis, which is a proton (H^+) consuming process, and by NH_3

Modelling ammonia emission from urine patches

A. Móríng et al.

Title Page

Abstract

Introduction

Conclusions

References

Tables

Figures



Back

Close

Full Screen / Esc

Printer-friendly Version

Interactive Discussion



emission which is a proton producing process. The water budget is increased by rain water and the liquid content of urine, whilst it is decreased by soil evaporation. The model was coded in R (R Core Team, 2012) and the steps of the calculation are shown in Fig. 2.

2.1 Simulation of ammonia exchange flux

As urine deposition by grazing animals typically happens on vegetated surfaces of grassland we need to take into account the effect of vegetation on the total net NH_3 flux (F_t , calculating as emission minus deposition) over a urine patch. Therefore, an ideal model should capture not just the ground flux at the soil surface (F_g) (referred hereafter as “soil emission”), but also the exchange with foliage (F_f), including NH_3 deposition to water and waxes on the leaf surface (F_w) and the NH_3 exchange with stomata (F_{sto}).

To achieve this, we extended the framework of the two-layer canopy compensation point model (abbreviated in this paper to 2LCCPM) of Nemitz et al. (2001) (Fig. 3). The original exchange model calculates F_g assuming a bulk soil compensation point on the soil surface. Instead of calculating this compensation point, we derive the compensation point for our model soil pore (χ_p). To capture the constraint due to soil particles on NH_3 exchange with the soil, we added a soil resistance (R_{soil}) to the original framework.

Based on the analogy of electrical circuit, seven equations (Eqs. 1–7) can be derived to determine the five unknown fluxes ($F_t, F_g, F_f, F_w, F_{\text{sto}}$) and the two unknown compensation points (over the vegetation, χ_c , and over the whole canopy, χ_{z0}). Parametrising the resistances – aerodynamic (R_a) and quasi-laminar resistance (R_b) over the canopy, aerodynamic resistance within the canopy (R_{ac}), quasi-laminar resistance (R_{bg}) at the ground, soil resistance, resistance to water and wax on the leaf surface (R_w) and stomatal resistance (R_{sto}) – as well as calculating the compensation point in the soil pore and in the stomata (χ_{sto}), we get a solvable linear system of equations.

$$F_t = F_g + F_f \quad (1)$$

Modelling ammonia emission from urine patches

A. M3ring et al.

Title Page

Abstract

Introduction

Conclusions

References

Tables

Figures



Back

Close

Full Screen / Esc

Printer-friendly Version

Interactive Discussion



$$F_f = F_w + F_{sto} \quad (2)$$

$$F_t = \frac{\chi_{z_0} - \chi_a}{R_a} \quad (3)$$

$$F_g = \frac{\chi_p - \chi_{z_0}}{R_{ac} + R_{bg} + R_{soil}} \quad (4)$$

$$F_f = \frac{\chi_c - \chi_{z_0}}{R_b} \quad (5)$$

$$F_w = \frac{-\chi_c}{R_w} \quad (6)$$

$$F_{sto} = \frac{\chi_{sto} - \chi_c}{R_{sto}} \quad (7)$$

Assuming steady state in every time step (1 h) and taking the air concentration of ammonia high above the canopy (χ_a) from measurements, the system of equations was solved for every time step by using the solve function of R programming language.

2.2 Parametrisation of the resistances and stomatal compensation point (R_a , R_b , R_{ac} , R_{bg} , R_w , R_{sto} , χ_{sto})

The detailed parametrisation of the resistances and the stomatal compensation point can be found in Sect. S1 in the Supplement together with all the model constants (Table S1). Here we focus on the modifications and model assumptions we made for applying the 2LCCPM of Nemitz et al. (2001) in the GAG model.

In the original description of the 2LCCPM, Nemitz et al. gave a parametrisation for R_a as a function of u^* (friction velocity) and L (Monin–Obukhov length), which were measured in the original modelling study. In the absence of measurements to obtain u^* and L , parametrisation should be used (Eqs. S7 and S8, respectively). As these two parameters depend on each other, we applied iteration to calculate both. For R_b we applied the formula suggested by Nemitz et al., expressed by Eq. (S12).

Following Nemitz et al., R_{ac} was assumed to be inversely proportional to u^* ($R_{ac} = \alpha u^{*-1}$). Massad et al. (2010a) recommended values for parameter α for many surface types – including grass – as well as for all of the four seasons (Table S1). Nemitz et al. applied a parametrisation for R_{bg} (s m^{-1}) for oilseed rape (Eq. S13). As the approach for calculation of this resistance for grasslands is not widely discussed in the literature, we adapted the one for oilseed rape for grassland. In our model, soil emission is dependent also on R_{soil} , which is larger at least by one order of magnitude than any of the atmospheric resistances. Thus, our model is not highly sensitive to this approximation for R_{bg} (for detailed analysis of the model sensitivity see Sect. 5).

The cuticular resistance (R_w) describes the effect of the water film, forming on the waxy leaf surface, on the NH_3 absorption. The extent to which such a thin water layer is present affects the value of R_w ; however, NH_3 absorption is also dependent on the air concentration of the acidic components (especially SO_2). These compounds, decreasing the pH of the water film, favour NH_3 deposition (Flechard et al., 1999). The process is referred to as co-deposition of the different components. The modelling of this phenomenon requires the knowledge of the chemical composition of the atmosphere and substantially increases model complexity. For a simpler approach, R_w (s m^{-1} , Eq. 8) can be estimated as a function of relative humidity (RH, %). For this purpose – similarly also to Nemitz et al. (2001) – we used the formula from Massad et al. (2010a) (based on Sutton and Fowler, 1993) with the recommended parameters in the same study ($R_{w(\text{min})}$, minimal cuticular resistance and a for grassland as reported by Horváth et al., 2005):

$$R_w = R_{w(\text{min})} \times \exp(a(100 - \text{RH})) \quad (8)$$

In the original description of the 2LCCPM R_{sto} is parametrised based on Hicks et al. (1987). Instead of this, we used a more state-of-the-art approach. As in Massad et al. (2010a), the value of R_{sto} (s m^{-1} , Eq. 9) was derived from the stomatal resistance of ozone ($R_{sto}(\text{O}_3)$, s m^{-1}), taking into account the difference between the diffusivity of the two gases ($D_{\text{O}_3}/D_{\text{NH}_3} = 1/1.6$). On the other hand, we parametrised $R_{sto}(\text{O}_3)$

BGD

12, 10059–10113, 2015

Modelling ammonia emission from urine patches

A. M3ring et al.

Title Page

Abstract

Introduction

Conclusions

References

Tables

Figures



Back

Close

Full Screen / Esc

Printer-friendly Version

Interactive Discussion



The stomatal compensation point, as the equilibrium gaseous NH_3 concentration in the stomata, can be derived from the temperature dependent form of Henry's law for dissolution of NH_3 (R1 in Table S2) and the dissociation coefficient of NH_4^+ (R4 in Table S2). Nemitz et al. (2000) derived χ_{sto} (Eq. 14) as a function of temperature (K) and the emission potential of the stomata (Γ_{sto}), which equals to the ratio of the NH_4^+ and H^+ concentrations (mol dm^{-3}) in the apoplastic fluid in the stomatal cavity.

$$\chi_{\text{sto}} = \frac{161\,500}{T} \times \exp\left(\frac{-10\,380}{T}\right) \times \Gamma_{\text{sto}} \quad (14)$$

In the original 2LCCPM Γ_{sto} is an input parameter from measurements. Since the measurement of Γ_{sto} is very difficult, in models it is usually handled as a constant, parametrised or simulated by a sub-model (e.g. Massad et al., 2010b; Wu et al., 2009). As over a urine patch NH_3 exchange is dominated by soil emission, we chose the parametrisation recommended by Massad et al. (2010a) for grazed fields. Equation (15) assumes that Γ_{sto} reaches its maximum $\Gamma_{\text{sto}}(\text{max})$ right after N application (in this case after urine deposition), and then decays exponentially with time (t_i indicates the time step, the hours spent after urine deposition, with a decay parameter τ set at 2.88×24 h).

$$\Gamma_{\text{sto}}(t_i) = \Gamma_{\text{sto}}(\text{max}) \times \exp\left(-\frac{t_i - 1}{\tau}\right) \quad (15)$$

$\Gamma_{\text{sto}}(\text{max})$ (Eq. 16), from Massad et al., 2010a, is determined by the amount of nitrogen applied (N_{app} , in kgN ha^{-1} , see Eq. 17), which in our case is the nitrogen content of the urine calculated as the volume of urine (W_{urine} , dm^3) multiplied by its nitrogen content (c_{N} , gN dm^{-3}), divided by the area of the urine patch (A_{patch} , m^2) (with 10 as a conversion factor between the different units).

$$\Gamma_{\text{sto}}(\text{max}) = 12.3 \times N_{\text{app}} + 20.3 \quad (16)$$

$$N_{\text{app}} = \frac{W_{\text{urine}} \times C_{\text{N}}}{A_{\text{patch}}} \times 10 \quad (17)$$

2.3 Simulation of the soil pore (χ_p) compensation point and the soil resistance (R_{soil})

The simulation of χ_p (mol dm^{-3}) is very similar in theory to that of χ_{sto} , being derived from Henry's law for NH_3 dissolution and the dissociation coefficient of NH_4^+ . In this way we get Eq. (18) (Nemitz et al., 2000), where T_{soil} is the soil temperature (K) and Γ_p is the ratio of the NH_4^+ and H^+ concentration in the model soil pore. In Eq. (19) Γ_p is expressed as a function of TAN concentration ($[\text{TAN}] = [\text{NH}_4^+] + [\text{NH}_3(\text{aq})]$) based on the definition of dissociation constant ($K(\text{NH}_4^+)$, second column of Table S2 and its temperature dependent form in the third column).

$$\chi_p = \frac{161\,500}{T_{\text{soil}}} \times \exp\left(\frac{-10\,380}{T_{\text{soil}}}\right) \times \Gamma_p \quad (18)$$

$$\Gamma_p = \frac{[\text{TAN}]}{K(\text{NH}_4^+) + [\text{H}^+]} \quad (19)$$

TAN and H^+ concentration (both in mol dm^{-3}) are derived from TAN budget (B_{TAN} , g N) and H^+ budget (B_{H^+} , mol), according to their mass ratio with water budget ($B_{\text{H}_2\text{O}}$, dm^3) (Eqs. 20 and 21, where 14 is the molar mass of nitrogen). All budgets are simulated within GAG (see B_{TAN} : Sect. 2.4, B_{H^+} : Sect. 2.6, and $B_{\text{H}_2\text{O}}$: Sect. 2.5).

$$[\text{TAN}] = \frac{\frac{B_{\text{TAN}}}{14}}{B_{\text{H}_2\text{O}}} \quad (20)$$

$$[\text{H}^+] = \frac{B_{\text{H}^+}}{B_{\text{H}_2\text{O}}} \quad (21)$$

For R_{soil} (s m^{-1}) we applied the approach by Laubach et al. (2012), as expressed in Eq. (22). This captures the effect of soil depth (Δz), that is, from how deep the soil NH_3 emission occurs on average. In the study of Laubach et al. Δz is referred as “source depth”, and in GAG model we consider it as the thickness of the source layer.

The inverse model experiments by Laubach et al. suggested that the distribution of Δz has a median of 0.002 m with an uncertainty factor of 2 and a similar value (0.003 m) was used in the study of Riedo et al. (2002) as well. In reality the thickness of the source layer changes parallel with the moisture content of the top soil layer; however, its approximation, due to the thinness of the layer, is difficult. Therefore, at the moment our model operates with a constant Δz of 0.004 m. (In Sect. 5.2 we tested the model sensitivity also to Δz .)

$$R_{\text{soil}} = \frac{\Delta z}{\xi D_g} \quad (22)$$

According to this approach, R_{soil} is inversely proportional to soil tortuosity (ξ) and diffusivity of NH_3 (D_g). For ξ , Laubach et al. (2012) suggested the parametrisation by Millington and Quirk (1961), based on the volumetric water content as well as porosity (θ_{por}):

$$\xi = \frac{(\theta_{\text{por}} - \theta)^{\frac{10}{3}}}{\theta_{\text{por}}^2} \quad (23)$$

2.4 Simulation of the TAN budget under the urine patch (B_{TAN})

The amount of TAN in the model soil pore in a given time step t_i ($B_{\text{TAN}}(t_i)$, g N), depends on its value in the previous time step ($B_{\text{TAN}}(t_{i-1})$, g N) and is controlled by the amount of TAN produced during urea hydrolysis (N_{prod} , g N) and soil NH_3 emission (F_g , g N m^{-2}) calculated in the previous time step (Eq. 24). We assume that B_{TAN} before

Title Page

Abstract

Introduction

Conclusions

References

Tables

Figures



Back

Close

Full Screen / Esc

Printer-friendly Version

Interactive Discussion



urine deposition is negligible small (compared to that of after urine deposition). Therefore, its initial value is set to 0. In the first time step (right after depositing urine), as well as if all the TAN was emitted as NH_3 in the previous time step, B_{TAN} equals to N_{prod} .

$$B_{\text{TAN}}(t_i) = \begin{cases} N_{\text{prod}}(t_i) & \text{if } (B_{\text{TAN}}(t_{i-1}) - F_g(t_{i-1}) \times A_{\text{patch}}) < 0 \\ N_{\text{prod}}(t_i) + B_{\text{TAN}}(t_{i-1}) - F_g(t_{i-1}) \times A_{\text{patch}} & \text{otherwise} \end{cases} \quad (24)$$

TAN production depends on the current amount of urea nitrogen within the model soil pore (B_{urea} , g N), as well as soil temperature (T_{soil} , °C). For N_{prod} Sherlock and Goh (1985) suggested an empirical formula (Eq. 25), with a temperature dependent parameter (A_h , Eq. 26) and a hydrolysis constant (k_h , see Table 1).

$$N_{\text{prod}}(t_i) = B_{\text{urea}}(t_i)(1 - \exp(A_h(t_i) \times k_h)) \quad (25)$$

$$A_h(t_i) = 0.25 \times \exp(0.0693 \times T_{\text{soil}}(t_i)) \quad (26)$$

Urea nitrogen content in a given time step (Eq. 27) is determined by its value in the previous time step, the loss as conversion to TAN ($-N_{\text{prod}}$) and, in the first time step, the amount of urea nitrogen added (U_{add} , g N) with the incoming urine. In U_{add} (Eq. 28) we take into account the dilution effect of rain and soil water on the nitrogen concentration of urine (c_n). We assume, that right after urine deposition the urea nitrogen content of urine, diluting in the total soil water ($B_{\text{H}_2\text{O}}^{\text{Tot}}$, Eq. 30), forms a homogenous soil solution with a concentration of c_n^{Tot} (Eq. 29). Finally, U_{add} is calculated as the product of c_n^{Tot} and the water content of the emission layer. (This will equal to $B_{\text{H}_2\text{O}}^{\text{Tot}}$ unless there is more water in the soil than can be stored in the emission layer, as indicated by $B_{\text{H}_2\text{O}}$ (max), which is specified in the following section, see Eq. 35).

$$B_{\text{urea}}(t_i) = B_{\text{urea}}(t_{i-1}) - N_{\text{prod}}(t_{i-1}) + U_{\text{add}}(t_i) \quad (27)$$

$$U_{\text{add}} = c_n^{\text{Tot}} \min\{B_{\text{H}_2\text{O}}(\text{max}), B_{\text{H}_2\text{O}}^{\text{Tot}}\} \quad (28)$$

Modelling ammonia emission from urine patches

A. Móríng et al.

Title Page

Abstract

Introduction

Conclusions

References

Tables

Figures



Back

Close

Full Screen / Esc

Printer-friendly Version

Interactive Discussion



$$C_n^{\text{Tot}} = C_n \frac{W_{\text{urine}}}{B_{\text{H}_2\text{O}}^{\text{Tot}}} \quad (29)$$

2.5 Simulation of the water budget under the urine patch ($B_{\text{H}_2\text{O}}^{\text{Tot}}$, θ , $B_{\text{H}_2\text{O}}$, $B_{\text{H}_2\text{O}}$ (max))

The soil moisture content affects NH_3 emission in several ways. In the first time step when the urine is deposited, both the water content of the model soil pore and the water content of the whole urine-affected soil layer ($B_{\text{H}_2\text{O}}^{\text{Tot}}$, Eq. 30) have an effect on emission. The thickness of the urine-affected soil layer depends on the amount of incoming liquids: urine (considering its whole volume as water) and rain (W_{rain} , dm^3). The more water is added, the more empty soil pore it can fill up and consequently, the deeper it will infiltrate.

We made the assumption for our model that the lowest possible volumetric water content in the soil is at permanent wilting point (θ_{pwp}) and the highest is at the field capacity (θ_{fc}), where both θ_{pwp} and θ_{fc} are expressed as fractions of total soil volume. Assuming that the initial soil water content is at θ_{pwp} , and after infiltration it rises to θ_{fc} , the volume fraction taken up by the incoming water will be $\theta_{\text{fc}} - \theta_{\text{pwp}}$. Finally, we get the total water content (incoming + soil water) in the urine-affected layer (having a volumetric water content of θ_{fc}) as:

$$B_{\text{H}_2\text{O}}^{\text{Tot}} = (W_{\text{rain}}(t_1) + W_{\text{urine}}) \frac{\theta_{\text{fc}}}{\theta_{\text{fc}} - \theta_{\text{pwp}}} \quad (30)$$

After urine deposition, actual volumetric water content (θ , Eq. 31) of the source layer can be expressed as the volume of the water in the layer ($B_{\text{H}_2\text{O}}$, dm^3) divided by the volume of the soil column under the urine patch with a surface area of A_{patch} (m^2) and

BGD

12, 10059–10113, 2015

Modelling ammonia emission from urine patches

A. M3ring et al.

Title Page

Abstract

Introduction

Conclusions

References

Tables

Figures



Back

Close

Full Screen / Esc

Printer-friendly Version

Interactive Discussion



a thickness of Δz (m) (in Eq. 31, 1000 is the conversion from m^3 to dm^3).

$$\theta = \frac{B_{\text{H}_2\text{O}}}{1000 \times \Delta z \times A_{\text{patch}}} \quad (31)$$

The actual water content of the soil at any time step ($B_{\text{H}_2\text{O}}'(t_i)$, Eq. 32) depends on the water content in the previous time step, soil evaporation (W_{evap} , dm^3), rain events (W_{rain} , dm^3) and in the very first time step the volume of urine (e.g. if the volume of the urine is 1.5 dm^3 then $W_{\text{urine}}(t_1) = 1.5 \text{ dm}^3$, otherwise 0). Both the volume of evaporation from the source layer and incoming rain to this layer are derived as the product of A_{patch} and soil evaporation (with E ($\text{dm}^3 \text{ m}^{-2}$): $W_{\text{evap}} = E \times A_{\text{patch}}$) as well as precipitation (with P ($\text{dm}^3 \text{ m}^{-2}$): $W_{\text{rain}} = P \times A_{\text{patch}}$) for a m^2 , respectively.

$$B_{\text{H}_2\text{O}}'(t_i) = \begin{cases} B_{\text{H}_2\text{O}}(\text{min}) + W_{\text{rain}}(t_i) + W_{\text{urine}}(t_i) & \text{if } (B_{\text{H}_2\text{O}}(t_{i-1}) - W_{\text{evap}}(t_{i-1})) < B_{\text{H}_2\text{O}}(\text{min}) \\ B_{\text{H}_2\text{O}}(t_{i-1}) - W_{\text{evap}}(t_{i-1}) + W_{\text{rain}}(t_i) + W_{\text{urine}}(t_i) & \text{otherwise} \end{cases} \quad (32)$$

It is not possible for more water to be evaporated from the source layer than the minimal water content (water content of the layer at θ_{pwp} : $B_{\text{H}_2\text{O}}(\text{min})$ (dm^3), Eq. 33). On the other hand, (as is shown in Eq. 34) this layer cannot store more water than the maximal water content (water content of the layer at θ_{fc} : $B_{\text{H}_2\text{O}}(\text{max})$ (dm^3), Eq. 35). The excess water is assumed to infiltrate to the deeper soil layers. (In Eqs. 33 and 35 1000 is the conversion from m^3 to dm^3 .)

$$B_{\text{H}_2\text{O}}(\text{min}) = 1000 \times \Delta z \times A_{\text{patch}} \times \theta_{\text{pwp}} \quad (33)$$

$$B_{\text{H}_2\text{O}}(t_i) = \min\{B_{\text{H}_2\text{O}}'(t_i), B_{\text{H}_2\text{O}}(\text{max})\} \quad (34)$$

$$B_{\text{H}_2\text{O}}(\text{max}) = 1000 \times \Delta z \times A_{\text{patch}} \times \theta_{\text{fc}} \quad (35)$$

Modelling ammonia emission from urine patches

A. M3ring et al.

Title Page

Abstract

Introduction

Conclusions

References

Tables

Figures



Back

Close

Full Screen / Esc

Printer-friendly Version

Interactive Discussion



no “deep percolation” (which occurs when θ exceeds θ_{fc} , but in our model θ_{fc} is assumed to be the maximum of θ).

- In the original approach it is assumed that soil evaporation attenuates when more water is evaporated from the soil evaporation layer (characterized by a thickness of Δz_E) than the amount of “readily evaporable water” (REW). The study of Allen et al. recommends REW values for different soil types defined by their θ_{fc} and θ_{pwp} . However, for the validation site of the present study (see Sect. 4.) with a sandy loam soil, these θ_{fc} and θ_{pwp} values were not in accordance with the measurements. Therefore we calculated REW as the water content of the evaporation layer halfway between θ_{fc} and θ_{pwp} :

$$REW = 1000(\theta_{fc} - 0.5(\theta_{fc} - \theta_{pwp})) \times \Delta z_E \quad (38)$$

The model constants used in the soil evaporation estimation are listed in Table S3.

2.6 Simulation of soil pH (B_{H^+})

After urine deposition, soil pH is affected by two main reactions: urea hydrolysis and NH_3 emission. When a urea molecule is decomposed an H^+ ion is consumed, producing two NH_4^+ ions and a bicarbonate ion (HCO_3^-). In the early stages of urea hydrolysis, when a large amount of urea is hydrolysed, a large amount of H^+ is required, resulting in a peak of soil pH (minimum of soil H^+ concentration). This triggers the dissociation of NH_4^+ and consequently the formation of gaseous ammonia, which also leads to an emission peak shortly after urine deposition. Once the majority of urea has been hydrolysed, ammonia emission may still be continuing. To balance the lost gaseous ammonia, more NH_4^+ dissociates, resulting in H^+ production, which tends to compensate the H^+ consumption associated with urea hydrolysis.

According to Sherlock and Goh (1985), after a rapid increase, soil pH usually peaks around 6–48 h after urine deposition (referred to as “first stage” of emission). Subsequently, the pH tends to drop for the reasons explained above over a period of about

Modelling ammonia emission from urine patches

A. M3ring et al.

Title Page

Abstract

Introduction

Conclusions

References

Tables

Figures



Back

Close

Full Screen / Esc

Printer-friendly Version

Interactive Discussion



2–8 days (second stage). Sherlock and Goh also identified two further stages: a 1–3 week long constant phase (third stage) when soil pH does not change considerably and, finally, a phase (fourth stage) with a moderate decline in soil pH, regulated by the nitrification of TAN.

As Sherlock and Goh (1985) pointed out that the bulk of TAN is volatilized over the first and second periods, and nitrification is a sufficiently slower process than NH_3 volatilization (see the cited references in the study of Sherlock and Goh), in the GAG model we neglect the effect of nitrification. On the other hand, we make the assumption that the solid material of soil is chemically inert, and consequently, NH_3 emission from soil is only affected by the composition of urine solution. To further focus our model onto the key reactions, we simulate urine chemistry considering only the water and urea available in the beginning, and the products of urea breakdown afterwards.

In this way, we consider the reactions for change of soil pH listed in Table S2: urea hydrolysis (R0), NH_4^+ dissociation (R1), dissociation of HCO_3^- and H_2CO_3 (carbonic acid) (R2 and R3, respectively), formation of gaseous NH_3 and CO_2 (carbon dioxide) (R4 and R5, respectively). However, considering that soil is a buffered system, we also incorporate a soil buffering capacity ($\beta \text{ mol H}^+ (\text{pH unit})^{-1} \text{ dm}^{-3}$). We defined β during test simulations with GAG. We found, that the model represents the measured pH the best with a β of $0.021 \text{ mol H}^+ (\text{pH unit})^{-1} \text{ dm}^{-3}$. To get the buffering effect in the volume of our model soil pore we calculated $\beta_{\text{patch}} = \beta \times A_{\text{patch}} \times \Delta z$. (For a sensitivity analysis to β see Sect. 5.3)

We defined 13 equations to calculate soil pH (Eqs. 39–51), eight of which are predictive equations, Eqs. (39)–(46), where B_X (mol) is the budget of the component X in the urine solution and r_{Rx} (mol) is the production or consumption of a given compound in reaction X . Variables i_N and i_C indicate the nitrogen and carbon input generated during urea hydrolysis, respectively. The nitrogen input is the same as N_{prod} but in mol ($i_N = N_{\text{prod}}/14$) and based on R0, $i_C = i_N/2$.

The other five equations describe the equilibrium in every time step (Eqs. 47–51). These were derived by reorganizing the equations in the second column in Table S2,

BGD

12, 10059–10113, 2015

Modelling ammonia emission from urine patches

A. M3ring et al.

Title Page

Abstract

Introduction

Conclusions

References

Tables

Figures



Back

Close

Full Screen / Esc

Printer-friendly Version

Interactive Discussion



where, for a dissolved component X : $[X] = B_x/B_{H_2O}$ and for a gaseous component $X_{(g)}$: $[X_{(g)}] = B_{X(g)}/V_{air}$. V_{air} is the volume of the air in the model soil pore, which can be calculated as the volume of the space in the model soil pore that is not taken up by the liquid content ($V_{air} = \theta_{por}A_{patch}\Delta z \times 1000 - B_{H_2O}$, where 1000 is the conversion between m^3 and dm^3).

Variables B_C and B_N represent the total inorganic carbon and nitrogen budget in the urine solution, respectively. Both can be derived as a sum of the different components and their input (by urea breakdown) and loss (via emission as gas) (Eqs. 52 and 53).

$$B_{H_2CO_3}(t_i) = B_{H_2CO_3}(t_{i-1}) + (-r_{R5} + r_{R3}) \quad (39)$$

$$B_{HCO_3^-}(t_i) = B_{HCO_3^-}(t_{i-1}) + (-r_{R2} - r_{R3} + i_C(t_i)) \quad (40)$$

$$B_{CO_3^{2-}}(t_i) = B_{CO_3^{2-}}(t_{i-1}) + r_{R2} \quad (41)$$

$$B_{CO_2(g)}(t_i) = B_{CO_2(g)}(t_{i-1}) + r_{R5} \quad (42)$$

$$B_{NH_4^+}(t_i) = B_{NH_4^+}(t_{i-1}) + (-r_{R1} + i_N(t_i)) \quad (43)$$

$$B_{NH_3(aq)}(t_i) = B_{NH_3(aq)}(t_{i-1}) + (r_{R1} - r_{R4}) \quad (44)$$

$$B_{NH_3(g)}(t_i) = B_{NH_3(g)}(t_{i-1}) + \left(r_{R4} - \frac{F_g(t_{i-1}) \times A_{patch}}{14} \right) \quad (45)$$

$$B_{H^+}(t_i) = B_{H^+}(t_{i-1}) - i_C(t_i) + (-r_{R3} + r_{R2} + r_{R1}) + \beta_{patch}(\text{pH}(t_i) - \text{pH}(t_{i-1})) \quad (46)$$

$$K(\text{NH}_4^+)(t_i)B_{H_2O}(t_i)B_{NH_4^+}(t_i) - B_{H^+}(t_i)B_{NH_3(aq)}(t_i) = 0 \quad (47)$$

$$K(\text{CO}_3^{2-})(t_i)B_{H_2O}(t_i)B_{HCO_3^-}(t_i) - B_{H^+}(t_i)B_{CO_3^{2-}}(t_i) = 0 \quad (48)$$

$$K(\text{H}_2\text{CO}_3)(t_i)B_{H_2O}(t_i)B_{H_2CO_3}(t_i) - B_{H^+}(t_i)B_{HCO_3^-}(t_i) = 0 \quad (49)$$

Modelling ammonia emission from urine patches

A. M3ring et al.

Title Page

Abstract

Introduction

Conclusions

References

Tables

Figures



Back

Close

Full Screen / Esc

Printer-friendly Version

Interactive Discussion



$$\left(H(\text{CO}_{2(\text{g})})(t_i) \frac{B_{\text{H}_2\text{O}}(t_i)}{V_{\text{air}}(t_i)} + 1 \right) B_{\text{H}_2\text{CO}_3}(t_i) + H(\text{CO}_{2(\text{g})})(t_i) \frac{B_{\text{H}_2\text{O}}(t_i)}{V_{\text{air}}(t_i)} B_{\text{HCO}_3^-}(t_i) + H(\text{CO}_{2(\text{g})})(t_i) \frac{B_{\text{H}_2\text{O}}(t_i)}{V_{\text{air}}(t_i)} B_{\text{CO}_2}(t_i) = H(\text{CO}_{2(\text{g})})(t_i) \frac{B_{\text{H}_2\text{O}}(t_i)}{V_{\text{air}}(t_i)} B_{\text{C}}(t_i) \quad (50)$$

$$\left(H(\text{NH}_{3(\text{g})})(t_i) \frac{B_{\text{H}_2\text{O}}(t_i)}{V_{\text{air}}(t_i)} + 1 \right) B_{\text{NH}_{3(\text{aq})}}(t_i) + H(\text{NH}_{3(\text{g})})(t_i) \frac{B_{\text{H}_2\text{O}}(t_i)}{V_{\text{air}}(t_i)} B_{\text{NH}_4^+}(t_i) = H(\text{NH}_{3(\text{g})})(t_i) \frac{B_{\text{H}_2\text{O}}(t_i)}{V_{\text{air}}(t_i)} B_{\text{N}}(t_i) \quad (51)$$

$$B_{\text{C}}(t_i) = B_{\text{H}_2\text{CO}_3}(t_{i-1}) + B_{\text{HCO}_3^-}(t_{i-1}) + B_{\text{CO}_3^{2-}}(t_{i-1}) + B_{\text{CO}_2}(t_{i-1}) + i_{\text{C}}(t_i) \quad (52)$$

$$B_{\text{N}}(t_i) = B_{\text{NH}_{3(\text{aq})}}(t_{i-1}) + B_{\text{NH}_4^+}(t_{i-1}) + B_{\text{NH}_3(\text{g})}(t_{i-1}) + i_{\text{N}}(t_i) - \frac{F_{\text{g}}(t_{i-1}) \times A_{\text{patch}}}{14} \quad (53)$$

Although references can be found in the literature for measurements of CO₂ emission from urine patches (e.g. Wang et al., 2013; Ma et al., 2006, and Lin et al., 2009), we considered that the driving processes behind them are not well-enough described for an hourly model application. Therefore, in the case of carbon budget we assumed no CO₂ emission in the basic GAG model, but we tested the effect of CO₂ emission in Sect. 5.3. The dissociation coefficients ($K(X)(t_i)$) and Henry constants ($H(X(\text{g}))(t_i)$) for the given t_i time step were derived as a function of actual soil temperature (third column of Table S2).

For a given $B_{\text{H}^+}(t_i)$ Eqs. (39)–(45) and (47)–(51) constitute a linear system of equations (12 equations, and seven $B_{\text{X}}(t_i)$ budgets and five r_{Rx} consumptions/productions as unknowns). As $B_{\text{H}^+}(t_i)$ is unknown, we are looking for a solution with a particular $B_{\text{H}^+}^*$ for this equation system, whose roots also satisfy Eq. (46), giving back $B_{\text{H}^+}^*$. For this purpose, we used the uniroot function of programming language R, which is able to look up this $B_{\text{H}^+}^*$. $B_{\text{H}^+}^*$ provides the H⁺ budget in the given time step and finally, pH can be calculated as $\text{pH} = -\lg(B_{\text{H}^+}^*/B_{\text{H}_2\text{O}})$.

Modelling ammonia emission from urine patches

A. Móríng et al.

Title Page

Abstract

Introduction

Conclusions

References

Tables

Figures

◀

▶

◀

▶

Back

Close

Full Screen / Esc

Printer-friendly Version

Interactive Discussion



3 Validation data

The GAG model described in the preceding sections was developed to simulate NH_3 emission from a single urine patch. However, for validation we chose a field experiment where the NH_3 emission flux was measured from several urine patches deposited relatively close in time. The only experiment we are aware of with these features was conducted by Laubach et al. (2012), who measured the NH_3 fluxes over a field covered with a regular pattern of urine patches.

In the experiment, 156 artificial urine patches were deposited within 45 min (see an overview of urine patch characteristics in Table 1) over a circular plot at an experimental site, in Lincoln New Zealand. In the middle of the plot NH_3 concentration was measured at five heights with Leuning samplers (Leuning et al., 1985) from which the fluxes were derived by different methods. For this study we used the fluxes calculated by Laubach et al. according to the mass balance (MB) method.

Soil samples were taken from 24 patches on the edge of the plot to measure soil pH, volumetric water content and mineral N content. Soil temperature was measured at two heights, and meteorological measurements were also carried out (from which we used wind speed, temperature, photosynthetically active radiation (PAR), sensible heat flux and atmospheric pressure data). For more details on measurements and flux calculation, see Laubach et al. (2012).

In addition to the available measurements, we also needed meteorological data that were not measured in the experiment: global radiation (R_{glob}) and RH. We obtained these data from the National Climate Database for New Zealand (NIWA, 2015).

We validated our model results against measurements of F_t , soil pH and θ for the measurement period between 24 February 2010, 11:30 a.m. and 1 March 2010, 1:30 a.m. In the case of F_t , the length of the collecting period of each measurement varied mostly between 1–1.5 h for daytime measurements, and 7–7.5 h for the nighttime measurements. As the time step of our model is 1 h and emission fluxes were not expected to change considerably over the night, we assumed that the measured aver-

BGD

12, 10059–10113, 2015

Modelling ammonia emission from urine patches

A. M3ring et al.

Title Page

Abstract

Introduction

Conclusions

References

Tables

Figures



Back

Close

Full Screen / Esc

Printer-friendly Version

Interactive Discussion



emission in the basic version of the model (see Sect. 5.3 for further examination of this effect).

Despite the large error bars on the measured mineral reduced soil N, its tendency is fairly similar to that of the TAN budget simulated by GAG. This is supported also by the significant correlation ($r = 0.63$) between the two parameters. The model performance in terms of volumetric water content is very good with a slight underestimation from the fourth day after urine application. The statistical analysis showed a high correlation of 0.92 at a 0.001 significance level.

Analysing the NH_3 emission, pH and TAN budget together, it can be concluded that the rain event affected all three parameters considerably. As it can be seen in the measured $\text{NH}_x\text{-N}$ and pH dataset (Fig. 4.), their values right after the rain event peaked close to the level (or even higher) of the first peaks, which were generated by urea hydrolysis. This suggests that urea breakdown might restart after the rain event, explaining the difference between the modelled and measured values.

The GAG model used here does not account for any retention of urine by vegetation; however, it is possible that this occurs in reality. For example, Doak (1952) found that the urine held on the leaf surfaces was 36 % of fresh herbage weight. In addition, the model assumptions do not allow the model soil pore to dry out (the minimum water content is at the permanent wilting point). In reality, however, the moisture content of urine retained on the leaf surfaces can evaporate easily and also some soil pores can completely dry out leaving behind the urine components undissolved. In such dry conditions, in lack of water urea hydrolysis stops. Then, after a rainfall, urea gets dissolved (as well as from the leaf surface it is washed into the soil) and hydrolysis can begin again, leading to a high peak in pH, TAN budget and consequently, NH_3 emission (see the further model results presented in Sect. S5).

BGD

12, 10059–10113, 2015

Modelling ammonia emission from urine patches

A. M3ring et al.

Title Page

Abstract

Introduction

Conclusions

References

Tables

Figures



Back

Close

Full Screen / Esc

Printer-friendly Version

Interactive Discussion



5 Sensitivity analysis for non-meteorological parameters

In the following subsections we investigated module by module (2LCCPM, TAN budget, soil pH and water budget), how the model responds if we change the most critical model features. In the case of the model constants, we tested how the modelled total emitted NH_3 (1.78 gN from a urine patch) changes over the modelling period by increasing and decreasing the given assumed model constant by 10 and 20 %. An overview of the results can be seen in Table 4. Comments on this table are provided in the following sections.

5.1 Sensitivity to atmospheric resistances

As the net NH_3 flux is dominated by the soil emission flux (shown in Fig. S1) we investigated here only the influence of the atmospheric resistances that affect the soil emission: R_{soil} , R_{bg} , R_{ac} and R_{a} . In Fig. 5, on the logarithmic scale it can be clearly seen that R_{ac} is the only atmospheric resistance that reaches the magnitude of the estimated R_{soil} .

For the simulation the main driver in temporal variation in R_{soil} is the actual volumetric water content (see Fig. 4). In the case of R_{a} , R_{b} , and R_{bg} there is at least an order of magnitude difference compared to the soil resistance, illustrating how the model performance is much less sensitive to the exact values of R_{a} , R_{ac} , and R_{bg} . The close temporal correlation of all these atmospheric resistances illustrates how they are all controlled by variations in wind speed and stability for a single canopy type. All the atmospheric resistances are the closest to the soil resistance when weak wind (large atmospheric resistances) is coupled to dry soil conditions (small soil resistance).

Among R_{bg} , R_{ac} and R_{a} , the parametrisation of R_{bg} is the most uncertain. As Table 4 shows, the model is hardly sensitive to the value of z_1 . In addition, u^*_{g} , as formulated by Nemitz et al. (2001), can also change in wide ranges without significantly affecting soil emission: R_{bg} could overcome the effect of R_{soil} on NH_3 emission only with a 10 times higher value of u^*_{g} .

5.2 Sensitivity to the estimation of the TAN budget

The two uncertain factors in the estimation of the TAN budget are the thickness of the source layer (Δz) and the area of the patch (A_{patch}). Originally the model was run with a Δz of 4 mm; however, the sensitivity analysis showed (Table 4) that the change in total emission is approximately half of the change in Δz . Therefore, this source of error must be considered when model results are evaluated.

We also tested the model with Δz values between the ranges reported by Laubach et al., 2012 (Fig. 6), and we found that the smaller the value of Δz , the higher is the emission peak after urine application and smaller are the emission peaks in the following days. Firstly, this is caused by a smaller value of R_{soil} , due to the thinner source layer. Secondly, since the thinner layer can store less TAN in total, the source layer runs out of TAN more quickly leading to lower peaks in the later part of the modelling period.

In addition, we carried out a simulation with the maximum value of Δz , the penetration depth of incoming urine. Considering that the water content of a y dm thick soil layer can be expressed as $A_{\text{patch}} \times y \times (\theta_{\text{fc}} - \theta_{\text{pwp}})$, the urine deposited in a single patch (W_{urine}) in this experiment will fill up a $y = 0.2 \text{ dm} = 20 \text{ mm}$ thick soil layer. In this case, R_{soil} is at least 5 times higher than in the original run (or even bigger as there is more water in the source layer consequently, the layer dries out more slowly), that prevents NH_3 from escaping from the soil shortly after urine deposition. However, from the second day due to the higher available TAN budget, the fluxes are closer to the measurements.

By contrast to Δz , the model does not appear to be very sensitive to A_{patch} , with even a +20% change causing less than 2% change in total emission (Table 4). Laubach et al. (2012) estimated that the patches gradually grew by lateral diffusion, so that the area of the patches had doubled over the modelling period at the validation site. Therefore, we conducted a simulation with GAG with a gradually growing patch, whose area doubles by the end of the period. In Fig. 7 we show the measured emission fluxes

BGD

12, 10059–10113, 2015

Modelling ammonia emission from urine patches

A. M3ring et al.

Title Page

Abstract

Introduction

Conclusions

References

Tables

Figures

⏪

⏩

◀

▶

Back

Close

Full Screen / Esc

Printer-friendly Version

Interactive Discussion



in relation to constant and gradually increasing values of A_{patch} , with the model results expressed for the whole area ($F_t(t_i) = F_t^{\text{single}}(t_i) \times (156 \times A_{\text{patch}}(t_i))/804.9$).

The largest difference with the growing patches, compared with the original run, occurred over the first two days. Then, the emission rates became smaller for the growing patches than with the constant patch area. The difference is a consequence of the combined effect of the growing source area ($156 \times A_{\text{patch}}(t_i)$) and the changing emission flux from a single patch.

In our model if a urine patch grows, it means physically that the initial liquid content is diffusing in the soil horizontally, leading to gradually declining volumetric water content. In addition, the evaporating area grows simultaneously, further intensifying the decrease of water content. Thus, R_{soil} will be smaller allowing stronger NH_3 emissions in the first two days. This leads to lower TAN budget in the second half of the period, resulting in slightly smaller emissions than in the original run.

5.3 Uncertainties in the estimation of soil pH

The main uncertainty in the model pH calculation is the applied buffering capacity (β). Apparently, the model is not highly sensitive to the tested changes of β ; however, using the same β for every soil type could lead to errors in NH_3 emission estimation. Therefore, we tested the model with two contrasting assumptions about buffering capacity: (a) when the system is totally buffered (pH is constant) and (b) when there is not any buffering effect ($\beta = 0$). For the constant pH scenario, we chose the soil pH measured before the deposition of the urine patches (pH = 6.65).

The results show (Fig. 8) that with a constant soil pH, GAG fails to capture the first, dominant peak in emission. This suggests that online modelling of pH is necessary for a proper estimation of NH_3 emission. By contrast, with $\beta = 0$ the model overestimates the first emission peak, while there is little difference in NH_3 fluxes in the rest of the period. Thus, with $\beta = 0$ the model is still capable of reproducing the daily cycle of NH_3 emission.

BGD

12, 10059–10113, 2015

Modelling ammonia emission from urine patches

A. M3ring et al.

Title Page

Abstract

Introduction

Conclusions

References

Tables

Figures

◀

▶

◀

▶

Back

Close

Full Screen / Esc

Printer-friendly Version

Interactive Discussion



Modelling ammonia emission from urine patches

A. Móríng et al.

Title Page

Abstract

Introduction

Conclusions

References

Tables

Figures



Back

Close

Full Screen / Esc

Printer-friendly Version

Interactive Discussion



Another feature of the model which affects the pH as well as the emission flux calculation is the handling of CO₂ emission following urine deposition (as discussed in Sect. 2.6). This is also suggested by the sudden drop in simulated pH at the beginning of the rain event (Fig. 4b) which seems to disappear if there is no rainfall over the modelling period (Fig. 9a, blue line).

At the beginning of the rainfall the volume of the gaseous part of the model soil pore suddenly shrinks as the liquid part grows with the incoming water. As a result (given that the base model does not allow CO₂ emission), gaseous CO₂ accumulates in the soil pore and is forced to dissolve into the liquid phase. This intensifies the formation of carbonic acid and its subsequent dissociation, leading to significant drop in pH.

In the experiment by Wang et al. (2013) CO₂ emission over urine patches peaked within 8 h after urine application, while both Ma et al. (2006) and Lin et al. (2009) found that the first peak of CO₂ emission occurred on the first day. In addition, Lin et al. (2009) reported a high correlation ($r = 0.63$) between CO₂ emission and soil temperature, suggesting a strong temperature dependency (similarly, we found a correlation of 0.58 for NH₃, see Table 5).

Based on the above similarities between the temporal development of NH₃ and CO₂ emission, to test the effect of CO₂ emission on the GAG simulations, we assumed that the amount of emitted CO₂ is half of the emitted NH₃ in moles (similarly to urea hydrolysis where from one urea molecule two NH₄⁺ and one HCO₃⁻ ions are produced). Even if this is a simplification for CO₂ emission, the results show the potential of future more comprehensive incorporation of the process into the model. By accounting for CO₂ emission the modelled pH values were found to be closer to the measured ones, while the sudden drop at the start of the rain event also largely disappeared (Fig. 9). As a consequence of these changes, the NH₃ emission fluxes were larger before the second day and – due to the larger loss in TAN budget – were smaller in the latter part of the experiment.

The apparently contradictory results with the assumed CO₂ emission above – better agreement in pH and poorer agreement in the NH₃ fluxes – suggest that the TAN in

the model soil pore is depleted too early, leading to a significant underestimation of the emission fluxes in the second part of the modelling period. Two scenarios can be envisaged that could cause this effect: scenario (1) the simulated rate of urea hydrolysis is higher than it is in reality, or scenario (2) at the experimental site fresh urea that had been intercepted by leaves and dried onto leaf surfaces, was washed to the soil during the rain event, thereby maintaining NH_3 emission afterwards.

As we discussed in Sect. 4, the measurement data also suggest the feasibility of scenario 2. Therefore, we tested the model – assuming that 10% of the applied urine was intercepted on the leaf surface – with 1.5 g of urea washed in during the rain event (see Sect. S5 in the Supplement). The simulation resulting from this assumption is consistent with the idea of the possible restart of breakdown of the fresh urea penetrating to the soil dissolved in rain water (for emission flux see Fig. 10d in Sect. 6, for TAN budget and pH see Fig. S2).

5.4 Uncertainties in the estimation of the water budget

The GAG model is found to be sensitive to model constants related to the water budget, especially field capacity, θ_{fc} (Table 4). The high sensitivity to a low value of θ_{fc} appears to be because this limits the amount of urine which remains available for hydrolysis and NH_3 emission from the source layer. In addition, we also found large differences in total ammonia emission when we modified the permanent wilting point. On regional scale it is not likely to have a database of measured θ_{fc} and θ_{pwp} values over a dense grid. It is more feasible that a soil texture map can be used for this purpose with recommended values of θ_{fc} and θ_{pwp} values for different soil types. Both θ_{fc} and θ_{pwp} can have an uncertainty of $\pm 20\%$ (e.g. in Allen et al. (1998) for sandy loam $\theta_{fc} = 0.18\text{--}0.28$), similarly to the extent of modification in the current sensitivity test. Therefore, at regional application, this uncertainty has to be considered when interpreting the model results.

BGD

12, 10059–10113, 2015

Modelling ammonia emission from urine patches

A. Möring et al.

Title Page

Abstract

Introduction

Conclusions

References

Tables

Figures



Back

Close

Full Screen / Esc

Printer-friendly Version

Interactive Discussion



6 Sensitivity to meteorological factors

For quantitative comparison, we show a variety of meteorological factors and the hourly NH_3 emission fluxes in Fig. 10. The NH_3 emission flux peaks almost every day shortly after midday, when soil temperature reaches its maximum. The only exception is the second day after urine application when the curve of emission flux stayed flat in the simulation, which was linked to the rain event as discussed in the previous sections.

The close relationship between the soil as well as the air temperature and NH_3 emission fluxes can be also seen in the calculated high correlations ($r = 0.58$ and $r = 0.60$, respectively). Compared with the other meteorological factors (Table 5) the relationship with these two seems to be the strongest. Relative humidity apparently has a slightly weaker, but still considerable role in the simulated NH_3 volatilization ($r = -0.49$). Based on the correlation values, there was a weaker relationship with wind speed ($r = 0.40$), which may be related to the fact that simulated R_{soil} provided a much larger constraint on NH_3 soil emission than the atmospheric resistances (Fig. 5). Global radiation as well as atmospheric pressure indicated a weaker influence (lower than $r = 0.40$ in absolute value) on the simulated NH_3 emission.

We also carried out a sensitivity analysis to the different meteorological parameters. To test the sensitivity to a given parameter, we modified it, while keeping all the other parameters the same, we ran a simulation with GAG. At the end of every simulation we calculated the total ammonia emission over the period, and expressed it as the percentage difference compared to the total emission in the original run. To get comparable results, we modified the original datasets in every case by $\pm\Delta x$, calculated as 10% of the difference between the measured minimum and maximum value of the given parameter over the modelling period.

Table 5 shows that NH_3 emission is the most sensitive to relative humidity (the differences in total emission were +9.1 and -8.6%) and wind speed (the differences were -5.5 and 4.7%). In addition, a relatively high difference (+4.1%) was observed in the case of global radiation when its values were raised by Δx .

BGD

12, 10059–10113, 2015

Modelling ammonia emission from urine patches

A. M3ring et al.

Title Page

Abstract

Introduction

Conclusions

References

Tables

Figures



Back

Close

Full Screen / Esc

Printer-friendly Version

Interactive Discussion



Modelling ammonia emission from urine patches

A. Móríng et al.

Title Page

Abstract

Introduction

Conclusions

References

Tables

Figures



Back

Close

Full Screen / Esc

Printer-friendly Version

Interactive Discussion



In spite of the high correlations, when soil and air temperature were modified separately, we got relatively small anomalies in the total emissions (less than 3% in absolute value for both soil and air temperature). However, when air and soil temperature were adjusted together (assuming that the change of these two temperature parameters is parallel), the differences were larger (see Table 5). Only low sensitivity was detected in the case of atmospheric pressure and hourly precipitation.

The results for wind speed and the different temperature parameters can be easily explained. Wind plays a governing role in turbulent mixing of the quasi-laminar and turbulent layer; consequently, it has a considerable effects on the vertical atmospheric transfer of ammonia. Regarding temperature, urea hydrolysis as well as the compensation point both in the stomata and the soil pores follow an exponential function of temperature.

Sutton et al. (2013) used a metric, Q_{10} , to express the relative increase in NH_3 emission over a range of 10°C . The combined temperature sensitivity presented in Table 5 amounts to around 3.31% change in emission per $^\circ\text{C}$ ($Q_1 = 1.0331$). Based on that $Q_{10} = Q_1^{10}$, according to our simulations, for a urine patch Q_{10} is going to be approximately 1.39. This value is rather smaller than the temperature dependencies for many volatilisation situations reviewed by Sutton et al. (2013). In the case of the GAG simulations, this relatively modest temperature response may in part results from altering the rapidity of emission, while constrained by the available TAN pool.

RH has a dual effect on NH_3 emission. Firstly, it plays a vital role in the water budget and secondly, it also influences the deposition of ammonia to the leaf surface. We tested the sensitivity in a model scenario where relative humidity was modified only in evaporation, and we observed only a +3.2% difference for $-\Delta x$ and -2.8% for $+\Delta x$ change. This clearly suggests that the effect of RH on NH_3 emission in GAG is stronger through deposition to leaf surfaces than through soil evaporation.

The physical explanation for the opposite change in RH and the total emission is that at higher values of relative humidity the formation of a water film on the leaf surface is more likely. As a result, deposition is more effective (see the different fluxes in Fig. S1),

which will generate a loss in the net emission flux over the whole system (including the exchange with soil and stomata as well as the deposition to cuticle).

Although precipitation was shown to suppress modelled emission, the total emission over the period was not strongly sensitive to a change of $\pm 10\%$ (± 0.08 mm) (Table 5).

This is a result of the model features that (1) allow only a $(\Delta z \times (\theta_{fc} - \theta_{pwp}) =) 1.2$ mm of maximum liquid content in the model soil pore and (2) do not allow wash out TAN from the source layer. Therefore, in the GAG model even a heavy rain event (> 6 mm h⁻¹) – apart from the slight effect on evaporation – has the same effect as a modest 1.2 mm h⁻¹ of precipitation. In the validation experiment during the rain event the soil reached its maximum water content (θ_{fc}). We found that by decreasing the amount of total precipitation so that the soil does not reach θ_{fc} , the maximum difference in total emission was +3%.

In addition, the timing of the rain event can also lead to a difference in total NH₃ emission due to the associated increase in R_{soil} which tends to suppress the rate of volatilization. We found that the timing of the rain event affects the NH₃ emission, with up to a 6% reduction or 2% increase in total NH₃ emission (see the model results in Sect. S6). Nevertheless, it must be emphasized that in reality NH₃ can escape from wet soil not only through gaseous diffusion in the empty soil pores. Dissolved NH₃ may get to the soil surface also through the solution and can be volatilized from there (Cooter et al., 2010). This is not taken into account in the present soil resistance parametrisation. Therefore, the effect of rainfall might not be as strong as this experiment showed. On the other hand, as we mentioned earlier, during a dry period urea hydrolysis may slow or stop in absence of water. If the rainfall begins after such a dry period, by restarting urea hydrolysis, it can even enhance ammonia emission rather than suppress it.

7 Conclusions

We constructed a novel NH₃ emission model for a urine patch (GAG) that is capable of simulating the TAN and the water content of the soil under a urine patch and also soil

BGD

12, 10059–10113, 2015

Modelling ammonia emission from urine patches

A. Móríng et al.

Title Page

Abstract

Introduction

Conclusions

References

Tables

Figures

◀

▶

◀

▶

Back

Close

Full Screen / Esc

Printer-friendly Version

Interactive Discussion



pH. According to the model validation, these are well represented by the model. The difference between the simulated and measured values suggested that to improve the model, further investigation is needed regarding the effect of a possible restart of urea hydrolysis with rain events.

5 The sensitivity analysis to the uncertain parameters showed that soil resistance had more than an order of magnitude stronger effect on soil NH_3 emission than the atmospheric resistances. An exceptional case is when weak wind is coupled with dry soil, in which case atmospheric and soil resistances may become comparable.

10 Our sensitivity analysis also showed that if the thickness of the source layer (Δz) is modified by a given percentage, the difference in the resulting total ammonia emission over the modelling period will be half of this percentage. Therefore, this source of error must be considered when model results are evaluated. Future work should also consider how independent datasets can help characterize the depth of the effective soil emission layer, as well as consider how both downward and upward migration of TAN with deeper soil layers can be addressed.

15 In the case of pH we showed that process-based modelling of pH is necessary to reproduce the very first high peak in NH_3 emission. The simulations were carried out with an assumed soil buffering capacity. While this affects the timing of emissions, we found that the total emission is not sensitive to the value of β and it is able to represent the main temporal development of ammonia emission even with 0 buffering capacity.

20 On the other hand, we found that incorporating a simple estimation of CO_2 emission allows the model to reproduce the measured soil pH values more accurately than neglecting CO_2 emissions. Future work should therefore consider how CO_2 fluxes could be incorporated more systematically into the GAG model.

25 The model turned out to be sensitive to the value of soil water content at field capacity (θ_{fc}) and at permanent wilting point (θ_{pwp}). Thus, at regional scale application, where mostly recommended values of these parameters are available, this error has to be considered when interpreting the model results.

BGD

12, 10059–10113, 2015

Modelling ammonia emission from urine patches

A. M3ring et al.

Title Page

Abstract

Introduction

Conclusions

References

Tables

Figures



Back

Close

Full Screen / Esc

Printer-friendly Version

Interactive Discussion



Modelling ammonia emission from urine patches

A. Móríng et al.

[Title Page](#)

[Abstract](#)

[Introduction](#)

[Conclusions](#)

[References](#)

[Tables](#)

[Figures](#)



[Back](#)

[Close](#)

[Full Screen / Esc](#)

[Printer-friendly Version](#)

[Interactive Discussion](#)



Our results support the vital role of temperature in NH_3 exchange, showing a high correlation with the temperature parameters as well as strong sensitivity to them. Nevertheless, the GAG model provides only a modest overall temperature dependence in total NH_3 emission compared with a review for several other surface types (Sutton et al., 2013). While temperature is clearly important in controlling diurnal dynamics within GAG, the overall emission rate is partly constrained by the TAN budget.

In addition, we found that wind speed and relative humidity are also significant influencing factors. In the case of RH we observed a dual effect through its effect on the modelled soil evaporation and the modelled deposition to leaf surfaces, with the latter being the dominant term for the present simulations.

As the model incorporates a canopy compensation point model it accounts for the effect of the meteorological parameters, providing a more realistic estimation for NH_3 exchange than the earlier NH_3 volatilization models for urea affected soils (Sherlock and Goh, 1985; Rachhpal and Nye, 1986). Compared to the model constructed by Laubach et al. (2012), GAG is capable of simulating the influence of vegetation on NH_3 exchange. In addition, our model also simulates soil pH, the TAN and the water content of the soil, allowing it to predict net NH_3 emission, instead of operating only in “inverse” mode, calculating soil parameters based on flux measurements.

Online simulation of soil pH is novel among the NH_3 exchange models on ecosystem scale. In the PaSim ecosystem model (Riedo et al., 2002) pH is treated as a constant, and the same is true for the VOLT’AIR model (Génermont and Cellier, 1997) developed for simulating NH_3 emission related to fertilizer and manure application. Furthermore, the framework of GAG is simpler and requires less input data than the VOLT’AIR model. Therefore, for grazing situations, it is much easier to adapt GAG on both field and regional scale.

Since all the input parameters can be obtained for larger scales, considering the possible errors, GAG is concluded to be suitable for larger scale application, such as in regional atmospheric and ecosystem models. In addition, as it is dynamically driven by

weather parameters, it can serve as a base for further studies of climate dependency of ammonia emission from grazed fields on both plot and regional scale.

**The Supplement related to this article is available online at
doi:10.5194/bgd-12-10059-2015-supplement.**

5 *Acknowledgements.* This work was carried out within the framework of the ÉCLAIRE project (Effects of Climate Change on Air Pollution and Response Strategies for European Ecosystems) funded by the EU's Seventh Framework Programme for Research and Technological Development (FP7).

References

- 10 Allen, R. G., Pereira, L. S., Raes, D., and Smith, M.: Crop Evapotranspiration – Guidelines for Computing Crop Water Requirements, FAO irrigation and drainage paper 56, FAO, Rome, Italy, 1998.
- 15 Burkhardt, J., Flechard, C. R., Gresens, F., Mattsson, M., Jongejan, P. A. C., Erisman, J. W., Weidinger, T., Meszaros, R., Nemitz, E., and Sutton, M. A.: Modelling the dynamic chemical interactions of atmospheric ammonia with leaf surface wetness in a managed grassland canopy, *Biogeosciences*, 6, 67–84, doi:10.5194/bg-6-67-2009, 2009.
- Cooter, E. J., Bash, J. O., Walker, J. T., Jones, M. R., and Robarge, W.: Estimation of NH₃ bi-directional flux from managed agricultural soils, *Atmos. Environ.*, 44, 2107–2115, doi:10.1016/j.atmosenv.2010.02.044, 2010.
- 20 Doak, B. W.: Some chemical changes in the nitrogenous constituents of urine when voided on pasture, *J. Agr. Sci.*, 42, 162–171, 1952.
- EDGAR: Emissions Database for Global Atmospheric Research v4.2, available at: <http://edgar.jrc.ec.europa.eu/> (last access: 20 May 2014), 2011.
- 25 Emberson, L., Simpson, D., Tuovinen, J.-P., Ashmore, M., and Cambridge, H.: Towards a Model of Ozone Deposition and Stomatal Uptake over Europe, EMEP MSC-W Note 6/2000, The Norwegian Meteorological Institute, Oslo, Norway, 2000.

Modelling ammonia emission from urine patches

A. Möring et al.

Title Page

Abstract

Introduction

Conclusions

References

Tables

Figures



Back

Close

Full Screen / Esc

Printer-friendly Version

Interactive Discussion



Modelling ammonia emission from urine patches

A. Móríng et al.

Title Page

Abstract

Introduction

Conclusions

References

Tables

Figures



Back

Close

Full Screen / Esc

Printer-friendly Version

Interactive Discussion



Laubach, J., Taghizadeh-Toosi, A., Sherlock, R. R., and Kelliher, F. M.: Measuring and modelling ammonia emissions from a regular pattern of cattle urine patches, *Agr. Forest Meteorol.*, 156, 1–17, doi:10.1016/j.agrformet.2011.12.007, 2012.

Laubach, J., Taghizadeh-Toosi, A., Gibbs, S. J., Sherlock, R. R., Kelliher, F. M., and Grover, S. P. P.: Ammonia emissions from cattle urine and dung excreted on pasture, *Biogeosciences*, 10, 327–338, doi:10.5194/bg-10-327-2013, 2013.

Leuning, R., Freney, J. R., Denmead, O. T., and Simpson, J. R.: A sampler for measuring atmospheric ammonia flux, *Atmos. Environ.*, 19, 1117–1124, doi:10.1016/0004-6981(85)90196-9, 1985.

Lin, X., Wang, S., Ma, X., Xu, G., Luo, C., Li, Y., Jiang, G., and Xie, Z.: Fluxes of CO₂, CH₄, and N₂O in an alpine meadow affected by yak excreta on the Qinghai-Tibetan plateau during summer grazing periods, *Soil Biol. Biochem.*, 41, 718–725, doi:10.1016/j.soilbio.2009.01.007, 2009.

Ma, X., Wang, S., Wang, Y., Jiang, G., and Nyren, P.: Short-term effects of sheep excrement on carbon dioxide, nitrous oxide and methane fluxes in typical grassland of Inner Mongolia, *New Zeal. J. Agr. Res.*, 49, 285–297, 2006.

Massad, R.-S., Nemitz, E., and Sutton, M. A.: Review and parameterisation of bi-directional ammonia exchange between vegetation and the atmosphere, *Atmos. Chem. Phys.*, 10, 10359–10386, doi:10.5194/acp-10-10359-2010, 2010a.

Massad, R.-S., Tuzet, A., Loubet, B., Perrier, A., and Cellier, P.: Model of Stomatal Ammonia Compensation Point (STAMP) in relation to the plant nitrogen and carbon metabolisms and environmental conditions, *Ecol. Model.*, 221, 479–494, doi:10.1016/j.ecolmodel.2009.10.029, 2010b.

Millington, R. J. and Quirk, J. P.: Permeability of porous solids, *T. Faraday Soc.*, 57, 1200–1207, doi:10.1039/TF9615701200, 1961.

Misselbrook, T. H., Gilhespy, S. L., Cardenas, L. M., Chambers, B. J., Smith, K. A., Williams, J., and Dragosits, U.: Inventory of Ammonia Emissions from UK Agriculture, Inventory Submission Report, DEFRA, London, UK, 2012.

Nemitz, E., Sutton, M. A., Schjoerring, J. K., Husted, S., and Paul Wyers, G.: Resistance modelling of ammonia exchange over oilseed rape, *Agr. Forest Meteorol.*, 105, 405–425, doi:10.1016/S0168-1923(00)00206-9, 2000.

Modelling ammonia emission from urine patches

A. Móríng et al.

Title Page

Abstract

Introduction

Conclusions

References

Tables

Figures



Back

Close

Full Screen / Esc

Printer-friendly Version

Interactive Discussion



Nemitz, E., Milford, C., and Sutton, M. A.: A two-layer canopy compensation point model for describing bi-directional biosphere–atmosphere exchange of ammonia, *Q. J. Roy. Meteor. Soc.*, 127, 815–833, doi:10.1256/smsqj.57305, 2001.

NIWA: The National Climate Database, available at: <http://cliflo.niwa.co.nz/>, last access: 2 December 2013, 2015.

Petersen, S. O., Sommer, S. G., Aaes, O., and Søgaard, K.: Ammonia losses from urine and dung of grazing cattle: effect of N intake, *Atmos. Environ.*, 32, 295–300, doi:10.1016/S1352-2310(97)00043-5, 1998.

Rachhpal, S. and Nye, P. H.: A model of ammonia volatilization from applied urea. I. Development of the model, *J. Soil Sci.*, 37, 9–20, doi:10.1111/j.1365-2389.1986.tb00002.x, 1986.

R Core Team: R: A language and environment for statistical computing, R Foundation for Statistical Computing, Vienna, Austria, 2012.

Riddick, S. N.: Global ammonia emissions from seabird colonies, Ph.D. thesis, Kings College, London, UK, 2012.

Riedo, M., Milford, C., Schmid, M., and Sutton, M. A.: Coupling soil–plant–atmosphere exchange of ammonia with ecosystem functioning in grasslands, *Ecol. Model.*, 158, 83–110, doi:10.1016/S0304-3800(02)00169-2, 2002.

Sherlock, R. R. and Goh, K. M.: Dynamics of ammonia volatilization from simulated urine patches and aqueous urea applied to pasture I. Field experiments, *Fert. Res.*, 5, 181–195, doi:10.1007/BF01052715, 1984.

Sherlock, R. R. and Goh, K. M.: Dynamics of ammonia volatilization from simulated urine patches and aqueous urea applied to pasture. II. Theoretical derivation of a simplified model, *Fert. Res.*, 6, 3–22, doi:10.1007/BF01058161, 1985.

Simpson, D., Benedictow, A., Berge, H., Bergström, R., Emberson, L. D., Fagerli, H., Flechard, C. R., Hayman, G. D., Gauss, M., Jonson, J. E., Jenkin, M. E., Nyíri, A., Richter, C., Semeena, V. S., Tsyro, S., Tuovinen, J.-P., Valdebenito, Á., and Wind, P.: The EMEP MSC-W chemical transport model – technical description, *Atmos. Chem. Phys.*, 12, 7825–7865, doi:10.5194/acp-12-7825-2012, 2012.

Sutton, M. A. and Fowler, D.: A model for inferring bi-directional fluxes of ammonia over plant canopies, in: *WMO Conference on the Measurement and Modeling of Atmospheric Composition Changes including Pollution Transport*, WMO/GAW-91, Sofia, Bulgaria, 04–08 October 1993, WMO, Geneva, 179–182, 1993.

Modelling ammonia emission from urine patches

A. Móríng et al.

Title Page

Abstract

Introduction

Conclusions

References

Tables

Figures



Back

Close

Full Screen / Esc

Printer-friendly Version

Interactive Discussion



- Sutton, M. A., Schjorring, J. K., and Wyers, G. P.: Plant–atmosphere exchange of ammonia, *Philos. T. Roy. Soc. A*, 351, 261–276, doi:10.1098/rsta.1995.0033, 1995.
- Sutton, M. A., Howard, C. M., Erisman, J. W., Bealey, W. J., Billen, G., Bleeker, A., Bouwman, A. F., Grennfelt, P., van Grinsven, H., and Grizzetti, B.: The challenge to integrate nitrogen science and policies: the European Nitrogen Assessment approach, in: *The European Nitrogen Assessment: Sources, Effects and Policy Perspectives*, edited by: Sutton, M. A., Howard, C. M., Erisman, J. W., Billen, G., Bleeker, A., Grennfelt, P., Van Grinsven, H., and Grizzetti, B., Cambridge University Press, Cambridge, UK, 82–96, 2011.
- Sutton, M. A., Reis, S., Riddick, S. N., Dragosits, U., Nemitz, E., Theobald, M. R., Tang, Y. S., Braban, C. F., Vieno, M., Dore, A. J., Mitchell, R. F., Wanless, S., Daunt, F., Fowler, D., Blackall, T. D., Milford, C., Flechard, C. R., Loubet, B., Massad, R., Cellier, P., Personne, E., Coheur, P. F., Clarisse, L., Van Damme, M., Ngadi, Y., Clerbaux, C., Skjøth, C. A., Geels, C., Hertel, O., Wichink Kruit, R. J., Pinder, R. W., Bash, J. O., Walker, J. T., Simpson, D., Horváth, L., Misselbrook, T. H., Bleeker, A., Dentener, F., and de Vries, W.: Towards a climate-dependent paradigm of ammonia emission and deposition, *Philos. T. Roy. Soc. B*, 368, 20130166, doi:10.1098/rstb.2013.0166, 2013.
- Walter, I., Allen, R., Elliott, R., Jensen, M., Itenfisu, D., Mecham, B., Howell, T., Snyder, R., Brown, P., Echings, S., Spofford, T., Hattendorf, M., Cuenca, R., Wright, J., and Martin, D.: ASCE's standardized reference evapotranspiration equation, in: *Watershed Management and Operations Management 2000*, American Society of Civil Engineers, Fort Collins, Colorado, US, 20–24 June 2000, 1–11, 2001.
- Wang, X., Huang, D., Zhang, Y., Chen, W., Wang, C., Yang, X., and Luo, W.: Dynamic changes of CH₄ and CO₂ emission from grazing sheep urine and dung patches in typical steppe, *Atmos. Environ.*, 79, 576–581, doi:10.1016/j.atmosenv.2013.07.003, 2013.
- Wu, Y., Walker, J., Schwede, D., Peterslidard, C., Dennis, R., and Robarge, W.: A new model of bi-directional ammonia exchange between the atmosphere and biosphere: ammonia stomatal compensation point, *Agr. Forest Meteorol.*, 149, 263–280, doi:10.1016/j.agrformet.2008.08.012, 2009.

Modelling ammonia emission from urine patches

A. Móríng et al.

Table 3. Model validation statistics: root mean square error (RMSE), correlation (r) and the level of significance of the correlation.

Variable	RMSE	Equation	r	Level of significance
Ammonia emission flux	43.06 $\mu\text{g N m}^{-2} \text{g}^{-1}$	$y = 34.63 + 0.50x$	0.54	0.01
Soil pH	0.56	$y = 3.04 + 0.64x$	0.75	0.001
Model TAN budget vs. measured soil $\text{NH}_x\text{-N}$	–	–	0.63	0.01
Soil water content	0.05	$y = 0.10 + 0.67x$	0.92	0.001

[Title Page](#)
[Abstract](#)
[Introduction](#)
[Conclusions](#)
[References](#)
[Tables](#)
[Figures](#)

[Back](#)
[Close](#)
[Full Screen / Esc](#)
[Printer-friendly Version](#)
[Interactive Discussion](#)


Modelling ammonia emission from urine patches

A. Móríng et al.

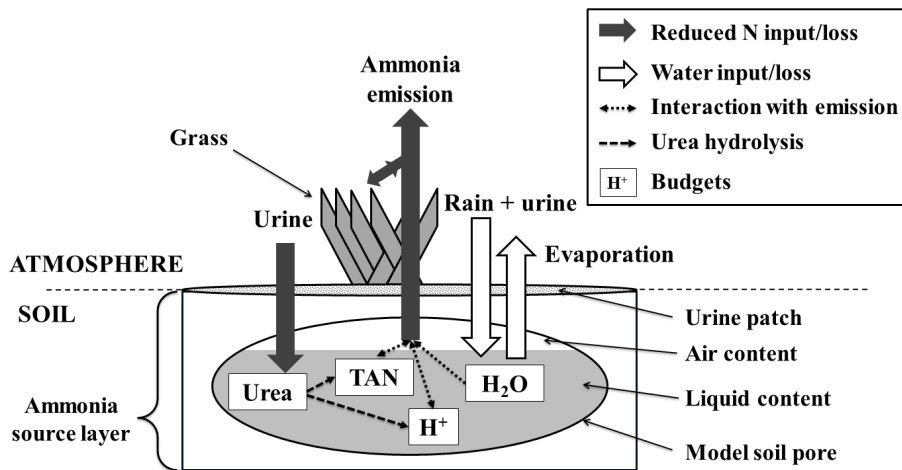


Figure 1. Schematic of major relationships in the GAG model.

Title Page

Abstract

Introduction

Conclusions

References

Tables

Figures

◀

▶

◀

▶

Back

Close

Full Screen / Esc

Printer-friendly Version

Interactive Discussion



Modelling ammonia emission from urine patches

A. Móríng et al.

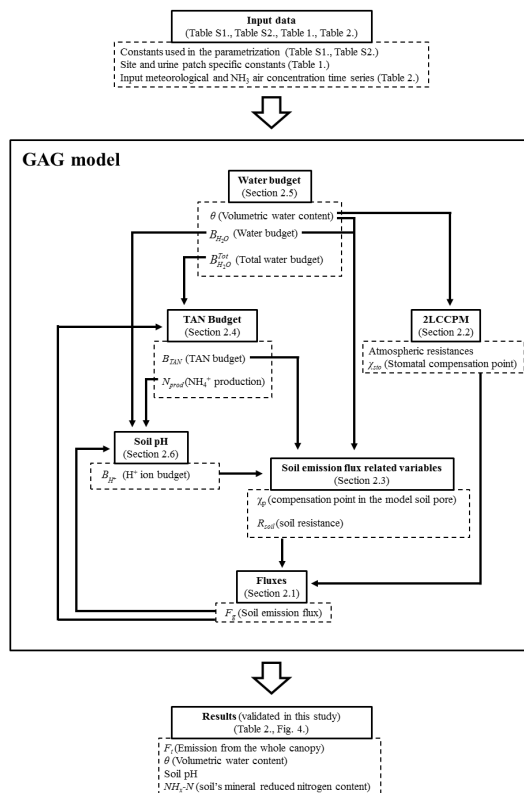


Figure 2. A flowchart depicting the steps of the calculation in the GAG model (middle panel), processing the input data (top panel) to the results that were validated in this study (bottom panel). The figure indicates the key variables that are carried from one module to another module(s). The figure, table and section numbers referred in the figure show where further description of the different model parts can be found in this paper. (2LCCPM stands for Two-Layer Canopy Compensation Point Model.)

Title Page

Abstract Introduction

Conclusions References

Tables Figures

◀ ▶

◀ ▶

Back Close

Full Screen / Esc

Printer-friendly Version

Interactive Discussion



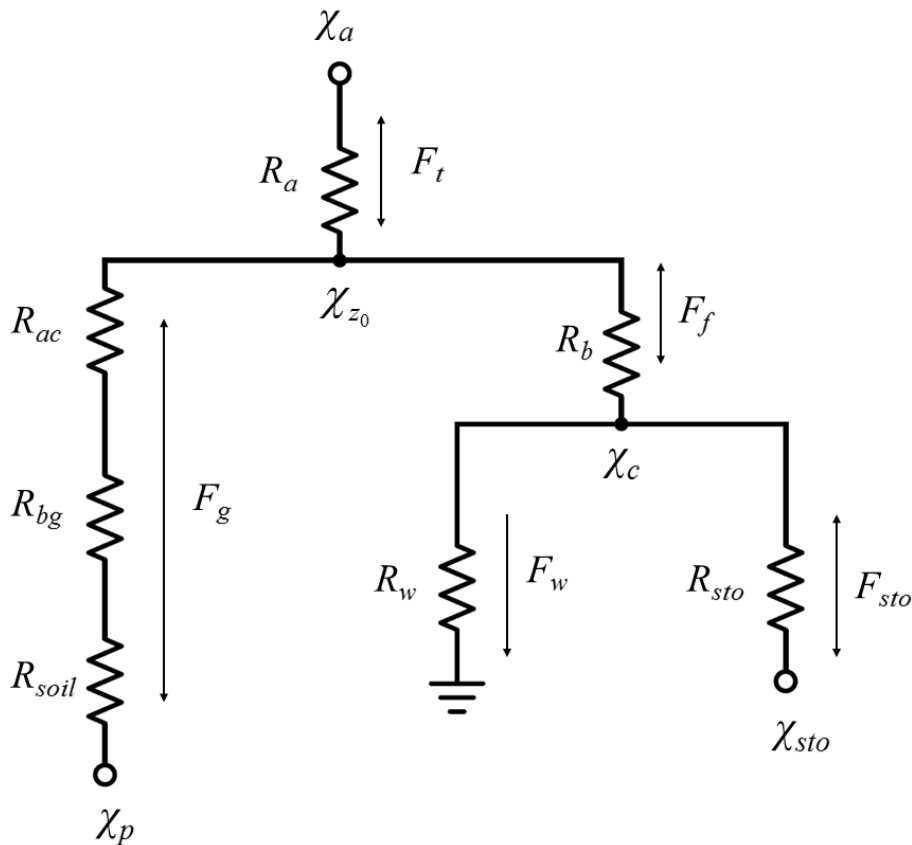


Figure 3. The network of gaseous resistances (R), ammonia concentrations (χ) and ammonia fluxes (F) used in the GAG model, which is based on the two-layer canopy compensation point model of Nemitz et al. (2001) incorporating concentration of the soil pore (χ_p) and soil resistance (R_{soil}). For the description of the other parameters in the framework see the text of this section.

Modelling ammonia emission from urine patches

A. M3ring et al.

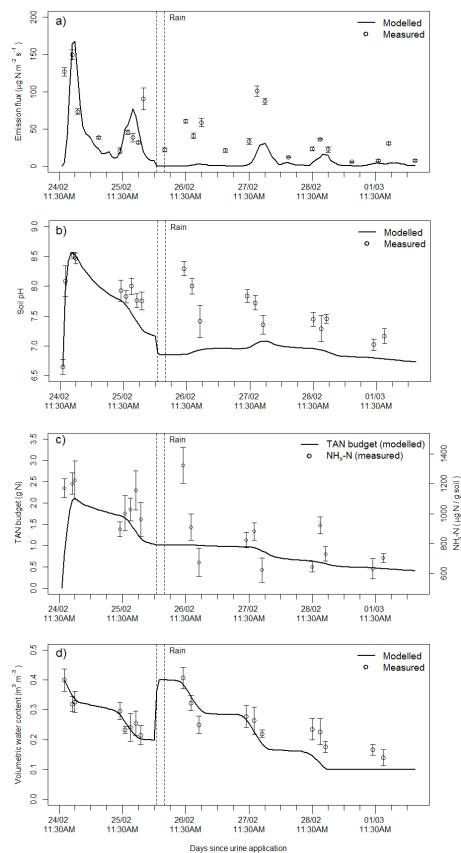


Figure 4. Comparison of modelled and measured values for NH₃ emission flux (a), soil pH (b), TAN budget and NH_x-N (c), and volumetric water content of the top 5 mm layer of the soil (d).

Modelling ammonia emission from urine patches

A. M3ring et al.

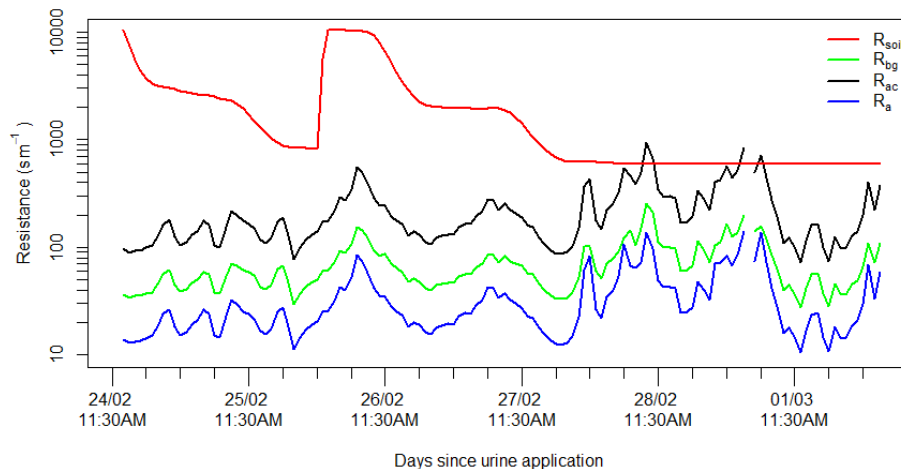


Figure 5. The atmospheric and the soil resistances over the modelling period. (At the time of the missing values in R_{bg} , R_{ac} and R_a u^* was 0, for which resistances are infinite. In these cases emission flux was assumed to be 0.)

Title Page

Abstract

Introduction

Conclusions

References

Tables

Figures



Back

Close

Full Screen / Esc

Printer-friendly Version

Interactive Discussion



Modelling ammonia emission from urine patches

A. M3ring et al.

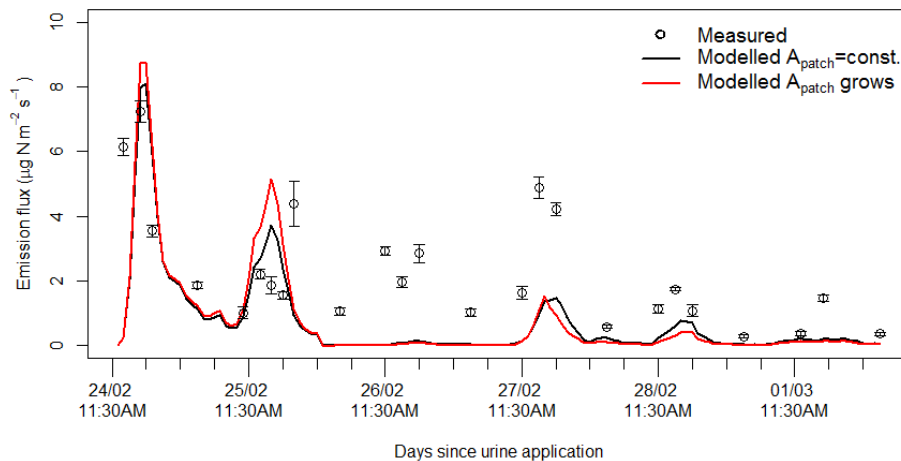


Figure 7. NH_3 fluxes from the whole experimental area with constant and with gradually growing urine patches.

[Title Page](#)[Abstract](#)[Introduction](#)[Conclusions](#)[References](#)[Tables](#)[Figures](#)[Back](#)[Close](#)[Full Screen / Esc](#)[Printer-friendly Version](#)[Interactive Discussion](#)

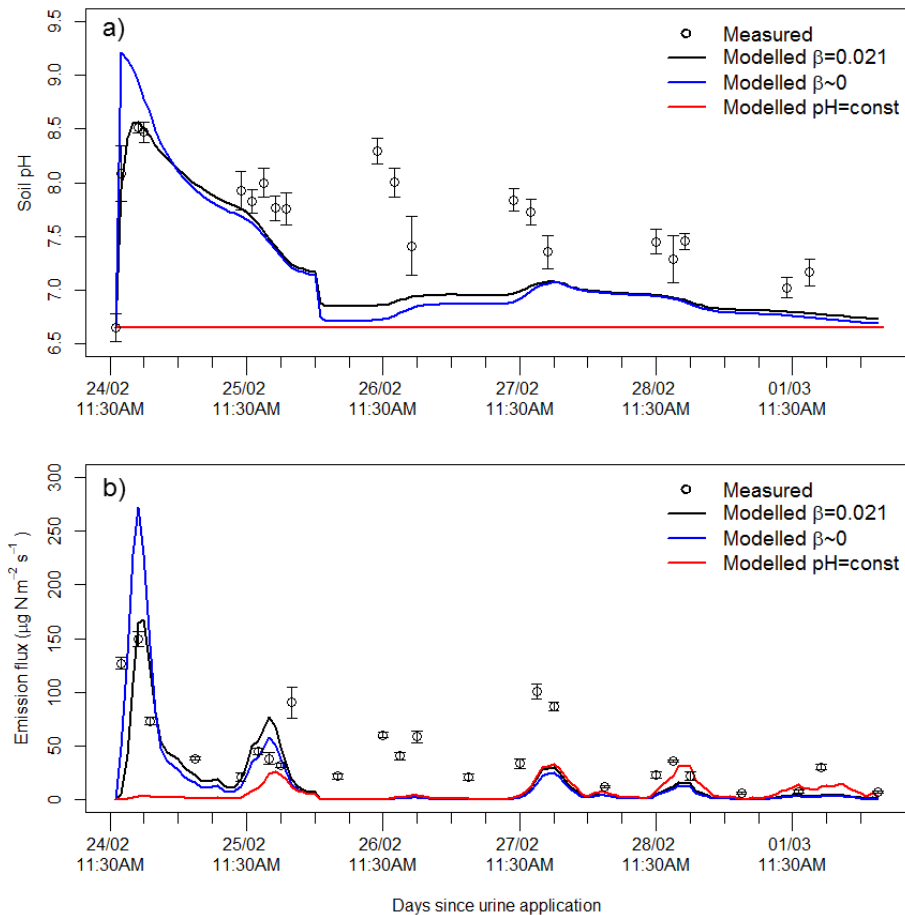


Figure 8. Soil pH under a urine patch **(a)** and NH_3 emission from it **(b)** with the currently applied buffering capacity ($\beta = 0.021$, original run), with no buffering ($\beta = 0$) and with constant pH, together with the measured values.

Modelling ammonia emission from urine patches

A. M3ring et al.

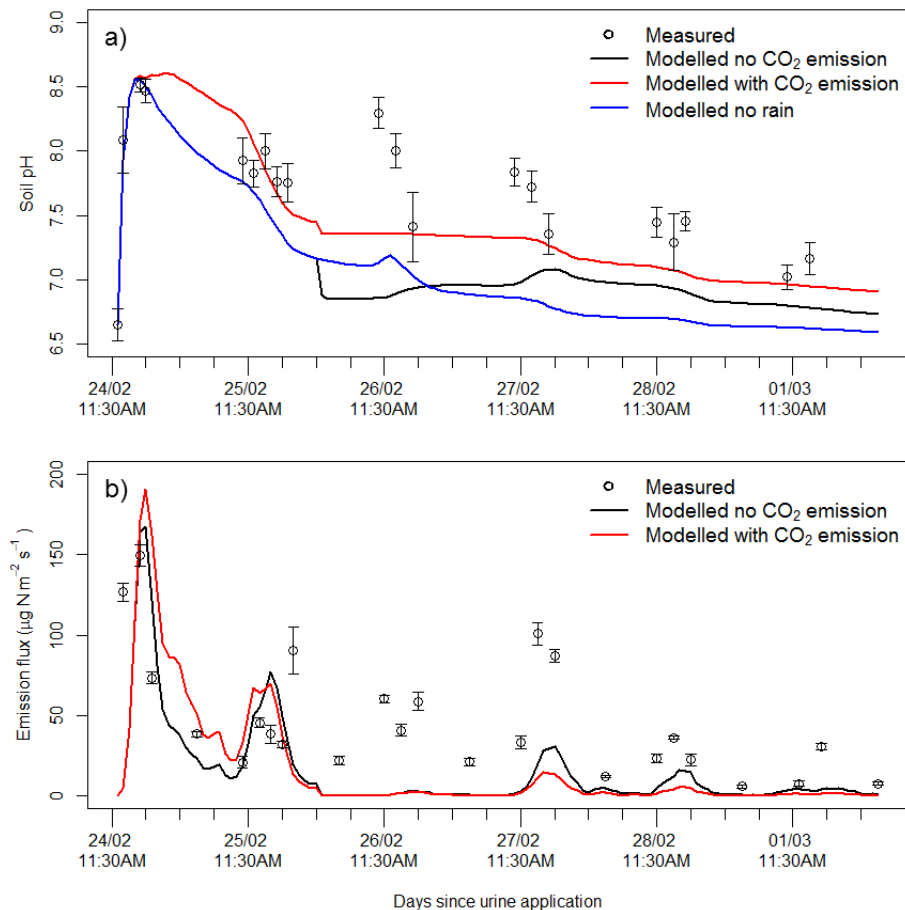


Figure 9. Soil pH under a urine patch (a) and NH₃ emission from it (b) without CO₂ emission (original run) and with an assumed CO₂ emission. On panel (a) the original run without rain is also plotted.

Modelling ammonia emission from urine patches

A. Móríng et al.

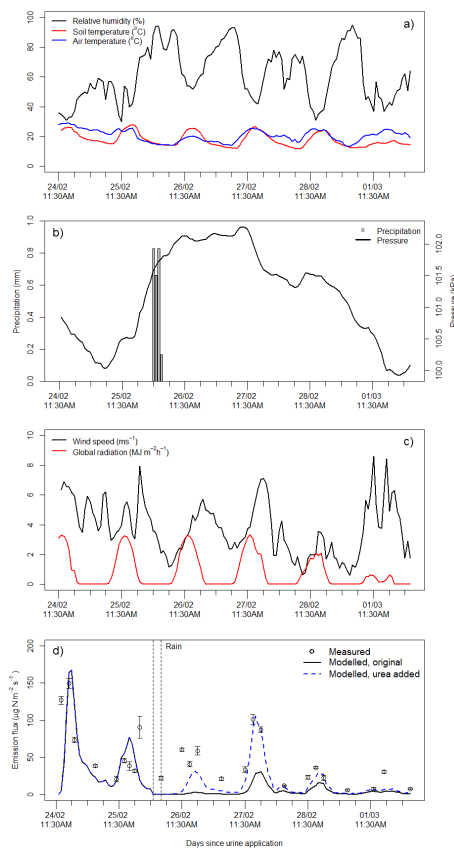


Figure 10. The investigated meteorological variables (relative humidity, soil and air temperature **(a)**, precipitation and surface pressure **(b)**, wind speed and global radiation **(c)**) and the hourly NH_3 fluxes **(d)** simulated by the original model (black line) and the modified model (dashed blue line), in which fresh urea was assumed to be washed into the soil during the rain event.

Title Page

Abstract

Introduction

Conclusions

References

Tables

Figures



Back

Close

Full Screen / Esc

Printer-friendly Version

Interactive Discussion

